Available online at www.sciencedirect.com

SCIENCE DIRECT®

ELSEVIER

Polymer 46 (2005) 7164–7175

polymer

www.elsevier.com/locate/polymer

Poly(vinylidene chloride-*co*-vinyl acetate): comprehensive microstructure analysis by NMR spectroscopy

Ajaib Singh Brar*, Gurmeet Singh, Ravi Shankar

Department of Chemistry, Indian Institute of Technology Delhi, Hauz Khas, New Delhi 110016, India

Received 19 January 2005; received in revised form 10 May 2005; accepted 22 May 2005
Available online 22 June 2005

Abstract

The microstructure analysis of poly(vinylidene chloride-*co*-vinyl acetate) was done using chemical shift modeling and 2D NMR spectroscopy. Chemical shift modeling was applied to analyze the compositional sensitive resonances of quaternary carbon of vinylidene chloride unit. Reactivity ratios determination was done from the diad and triad fractions. To resolve the complex ^{1}H and ^{13}C{^{1}H} NMR spectra of copolymers, 2D ^{1}H/^{13}C hetero-nuclear single quantum coherence (HSQC), ^{1}H/^{1}H total correlation spectroscopy (TOCSY) and hetero-nuclear multiple bond correlation (HMBC) experiments were conducted. The combination of 2D NMR experiments supported by chemical shift modeling enabled to assign the complex and overlapping proton and carbon-13 resonances unambiguously.

Keywords: NMR; HMBC; Modeling

1. Introduction

Nuclear magnetic resonance experiments contribute valuable structural information, helping in the deeper understanding of polymer properties and thus permitting synthesis of polymers with required properties [1–14]. 2D NMR has emerged as the most effective technique for the study of polymer structure. Rinaldi et al. have pioneered the application of the multi-dimensional NMR experiments for the analysis of polymers [1–3]. Application of 2D NMR techniques with special emphasis on hetero-nuclear correlation experiments has been followed by large, indicated by the large number of publications incorporating 2D NMR for the analysis of polymer structure [1–7].

Vinylidene chloride copolymers because of their gas and vapor impermeability, find applications as membranes in molding resins, rigid barrier containers, foams and etc. Microporous and mesoporous activated carbons obtained from vinylidene chloride copolymers act as effective adsorbent for water purification, gas separation and as support materials in catalysis systems [15–19]. In recent years, activated carbons from poly(vinylidene chloride) have started to find usage in energy storage devices such as in non-aqueous electric double layer capacitors and methane storage for fuel cells [19–21]. The microstructure analysis of the vinylidene copolymers can thus give a better insight to their physical properties.

In this paper, for the microstructure analysis of the poly(vinylidene chloride-*co*-vinyl acetate), a sequential approach based on the reactivity ratios determination, chemical shift modeling and 2D NMR spectral analysis is presented. Cheng et al. [22–24], Matlengiewicz et al. [25, 26] and Brar et al. [8,27,28] have applied the useful feature of additivity of carbon-13 NMR chemical shifts for the microstructure analysis of polymers. Combination of chemical shift modeling along with NMR spectral analysis enabled the apparent assignments of the complex proton and carbon-13 resonances. Analysis of the 2D TOCSY, HSQC and HMBC spectrum of a copolymer (of composition $F_V = 0.52$) enabled the complete assignment of the proton and carbon-13 resonances, thus eliminating the need of analyzing the spectra of copolymers of different compositions.

---

* Corresponding author. Tel.: +91 112 659 1377; fax: +91 112 658 1102.

E-mail address: asbrar@chemistry.iitd.ernet.in (A.S. Brar).

0032-3861/$ - see front matter © 2005 Elsevier Ltd. All rights reserved.
doi:10.1016/j.polymer.2005.05.088

2. Experimental

2.1. Synthesis of polymers

Vinylidene chloride (Fluka, Germany) and vinyl acetate (Merck, Germany) were distilled and stored at low temperature. Uranyl nitrate (Merck, Germany), the free radical photo-initiator was recrystallized from distilled methanol, dried and stored at low temperature. A series of vinylidene chloride (V)/vinyl acetate (A) copolymers were synthesized in bulk using uranyl nitrate as photo-initiator. The polymerization was stopped at low conversion by precipitating the reaction mixtures in large excess of methanol. Further purification was done using chloroform/methanol as solvent/precipitant system and the polymers were then dried in vacuum.

2.2. NMR experiments

1D and 2D NMR spectra were recorded on the Bruker DPX-300 spectrometer in $CDCl_3$. ^1H and ^{13}C measurements were made at frequencies of 300.13 and 75.5 MHz, respectively, and referenced with respect to the $CDCl_3$ solvent signal. Gradient HSQC and HMBC experiments were recorded using the pulse sequences invigpt and inv4gplplrnd of the Bruker software, respectively. The HSQC and HMBC spectra were acquired with 512 increments in the F1 dimension and 2048 data points in the F2 dimension. Four dummy scans and 32 scans were used for HSQC and HMBC spectral recording. Total correlation spectroscopy (TOCSY) experiment was performed using the standard pulse sequence. Thirty-two scans were accumulated for 512 experiments. For the ^{13}C and 2D NMR measurements 2 s delay time was used.

2.3. Calculations and NMR spectral simulation

Chemical shift modeling was done by using a model developed on the basis of the models proposed by Cheng et al. [22–24] and Matlengiewicz et al. [25,26]. Reactivity ratios optimization was done by modifying the least square residue approach proposed by van Herk et al. [29,30]. Details of the coding of Real Coded Genetic Algorithm (RCGA), reactivity ratios optimization, ^{13}C NMR chemical shift modeling and NMR spectral simulation are described in the earlier publications by Brar et al. [27,28]

3. Results and discussion

Fig. 1 shows the assigned $^{13}C\{^1H\}$ NMR and DEPT-135 NMR of vinylidene chloride (V)/vinyl acetate (A) copolymer of composition $F_V = 0.52$. The assignments were done by comparing with the $^{13}C\{^1H\}$ NMR spectrum of poly(vinyl acetate) [31] and vinylidene chloride copolymers [32,33]. Resonances around 21.5 ppm were assigned to the methyl group of vinyl acetate. The resonances around 40.0, 52.4 and 62.2 ppm were assigned to AA, AV and VV methylene diads, respectively, on comparing with the spectrum of poly(vinyl acetate) spectrum and by observing change in intensity of signals with composition. These assignments were further confirmed by the DEPT-135 NMR spectrum given in Fig. 1(b). Resonances around 67.0 ppm were assigned to the methine carbon of vinyl acetate. Signals around 170.3 ppm were assigned to the carbonyl carbon of vinyl acetate.

In $^{13}C\{^1H\}$ spectrum (Fig. 1(a)) region in the range of 89.0–82.2 ppm was assigned to the quaternary carbon of vinylidene chloride, with expansion given in Fig. 2(a). On analyzing change in the intensity of resonances as function of composition (Fig. 3(a)) the quaternary carbon resonances were assigned for compositional sensitivity. The peak 1, shown in Fig. 2(a) was assigned to VVV triad, the peaks 2, 3, 4 and 5 were assigned to AVV triad and peaks 6, 7 and 8 were assigned to AVA triad.

In the ^1H spectrum shown in Fig. 4 peak at 1.97 ppm was assigned to methyl protons of the vinyl acetate monomer unit. The resonances from 1.6 to 3.9 ppm were assigned to the methylene protons and resonances from 4.6 to 6.0 ppm were attributed to methine proton of the vinyl acetate unit. The assignments of the resonances are explained in the 2D NMR section of the paper.

3.1. Reactivity ratios determination

Five copolymer samples of different compositions, $F_V =$ 0.29, 0.39, 0.52, 0.71 and 0.79 were synthesized for the reactivity ratios determination of vinylidene chloride/vinyl acetate copolymers. From $^{13}C\{^1H\}$ NMR spectra, area under the AA, AV and VA diads was calculated for the five copolymers and normalized. From the diad fractions both the reactivity ratios were optimized using least square residue approach [28–30]. The optimized reactivity ratios were found to be $r_V = 5.80$ and $r_A = 0.057$. The experimental and theoretical diad fractions are shown in Fig. 5. The copolymer compositions are listed in Table 1. To check the reactivity ratios obtained from the diad fractions, the optimization was also carried from the triad fractions.

Reactivity ratio optimized for vinylidene chloride monomer unit in the copolymer system from the V centered VVV, AVV and AVA triad fractions obtained from the $^{13}C\{^1H\}$ spectra was $r_V = 5.65$. Triad fractions of the A centered AAA, AAV and VAV triads from the ^1H spectra of copolymers of different compositions were used to optimize

Table 1
Infeed (f_V) and outfeed (F_V) mole fraction of vinylidene chloride (V) in poly(vinylidene chloride-*co*-vinyl acetate) copolymerization

f_V	0.03	0.05	0.10	0.25	0.35
F_V	0.29	0.39	0.52	0.71	0.79

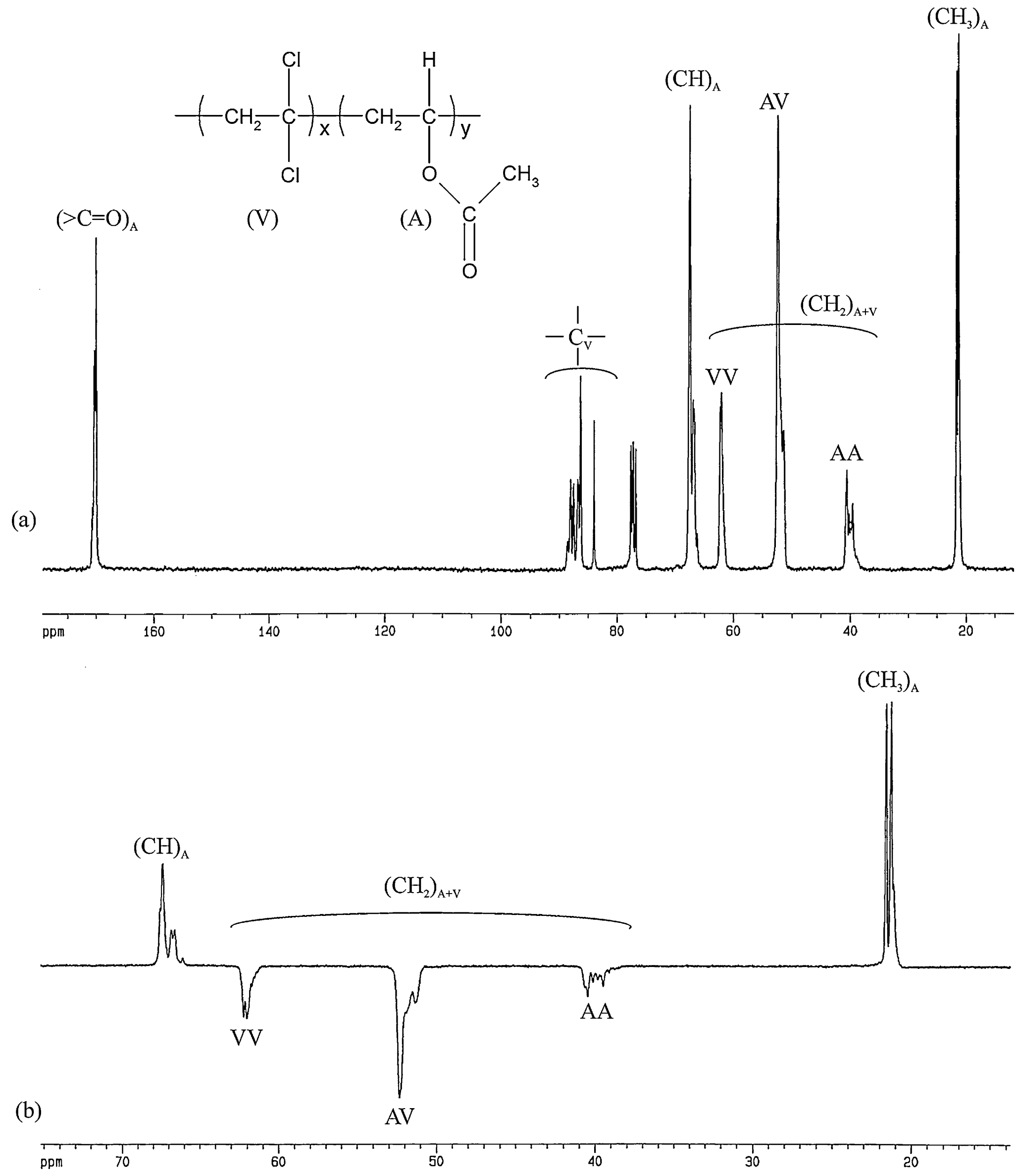

Fig. 1. Assigned spectra of poly(vinylidene chloride-*co*-vinyl acetate) of composition $F_V = 0.52$ (a) $^{13}C\{^1H\}$ NMR spectrum and (b) DEPT-135 spectrum.

the reactivity ratio for the vinyl acetate unit. r_A was calculated to be 0.061. As evident from the joint confidence interval shown in Fig. 6, the reactivity ratios obtained from the triad fractions were well with in the joint confidence interval for the reactivity ratios obtained from the diad fractions. Hence the results obtained from the diad and triad fractions were in good agreement.

3.2. NMR spectral simulation

The peak 1, shown in Fig. 2(a), at 83.98 ppm was assigned to VVV triad. The AVA triad was observed to be split in three regions, labeled as 6, 7 and 8 assigned to VAVAV, AAVAV and AAVAA pentads, respectively. AVV triad centered pentads constituted two broad resonance signals, thereby making the assignments of VAVVV, VAVVA, AAVVV and AAVVA pentads difficult. To resolve these resonances, a methodology based on the chemical shift prediction and spectral simulation was applied.

Empirical chemical shift modeling of the AVA triad centered VAVAV, AAVAV and AAVAA pentads and VVV triad was done. The empirical additive parameters were optimized using RCGA. The optimized additive parameters are given in Table 2. $^{13}C\{^1H\}$ NMR chemical shifts of VAVVV, VAVVA, AAVVV and AAVVA pentads were then calculated from the optimized parameters. Experimental and calculated chemical shift values are listed in Table 3. From the calculated chemical shifts it was concluded that peaks 2 and 3 (Fig. 2(a)) were due to VAVVV and VAVVA pentad sequences and peaks 4 and 5 were attributed to AAVVV and AAVVA pentads.

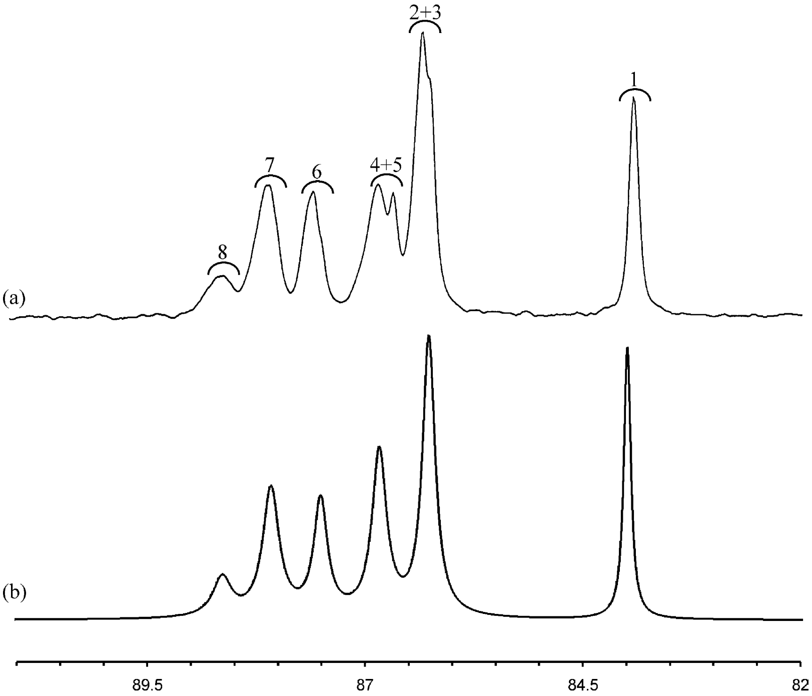

Fig. 2. $^{13}C\{^{1}H\}$ NMR spectra of quaternary carbon in poly(vinylidene chloride-*co*-vinyl acetate) of composition $F_V=0.52$ (a) observed spectrum and (b) simulated spectrum.

The experimental and theoretical V centered pentad fractions at different compositions are listed in Table 4. Good agreement between the experimental and theoretical data established that good estimate of reactivity ratios was obtained and substantiated the assignments. The simulation of NMR spectra of different compositions was done. Fig. 2 shows comparison of the experimental and simulated spectrum for copolymer of composition $F_V=0.52$. The experimental and theoretical NMR spectra of copolymers of different compositions are given in Fig. 3. Good match

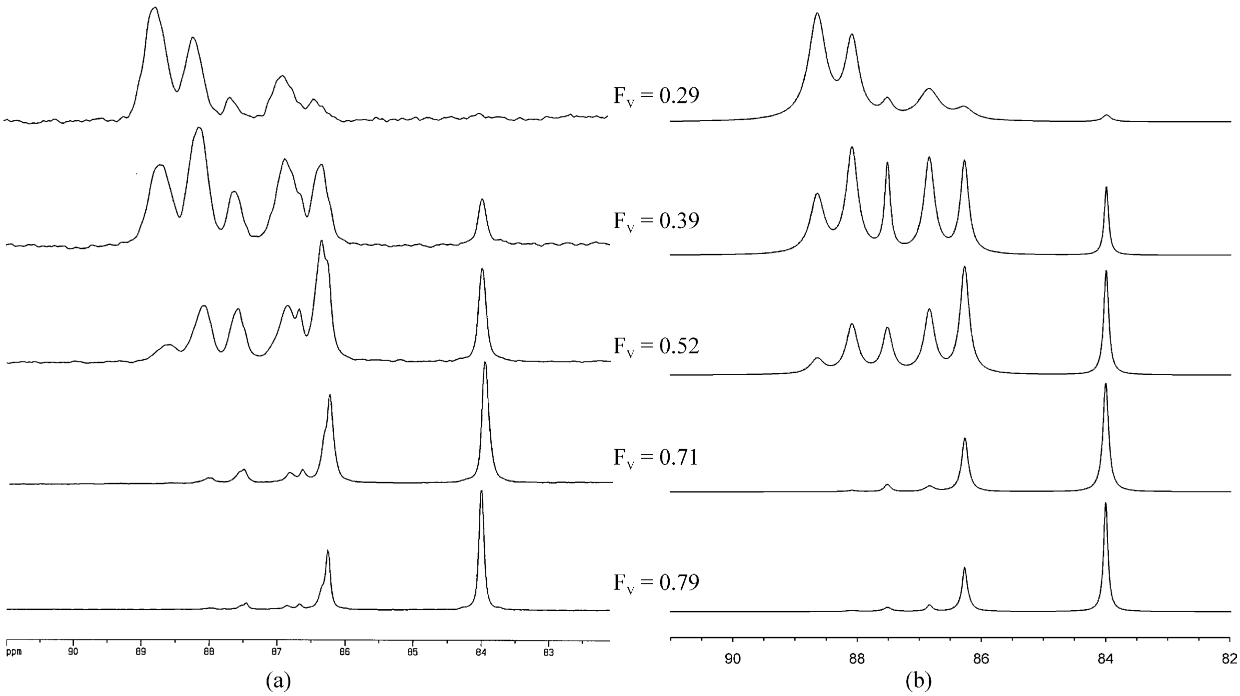

(a)

(b)

Fig. 3. $^{13}C\{^{1}H\}$ NMR spectra of quaternary carbon of vinylidene chloride in poly(vinylidene chloride-*co*-vinyl acetate) at different copolymer compositions (a) observed spectra and (b) simulated spectra with adjusted line widths.

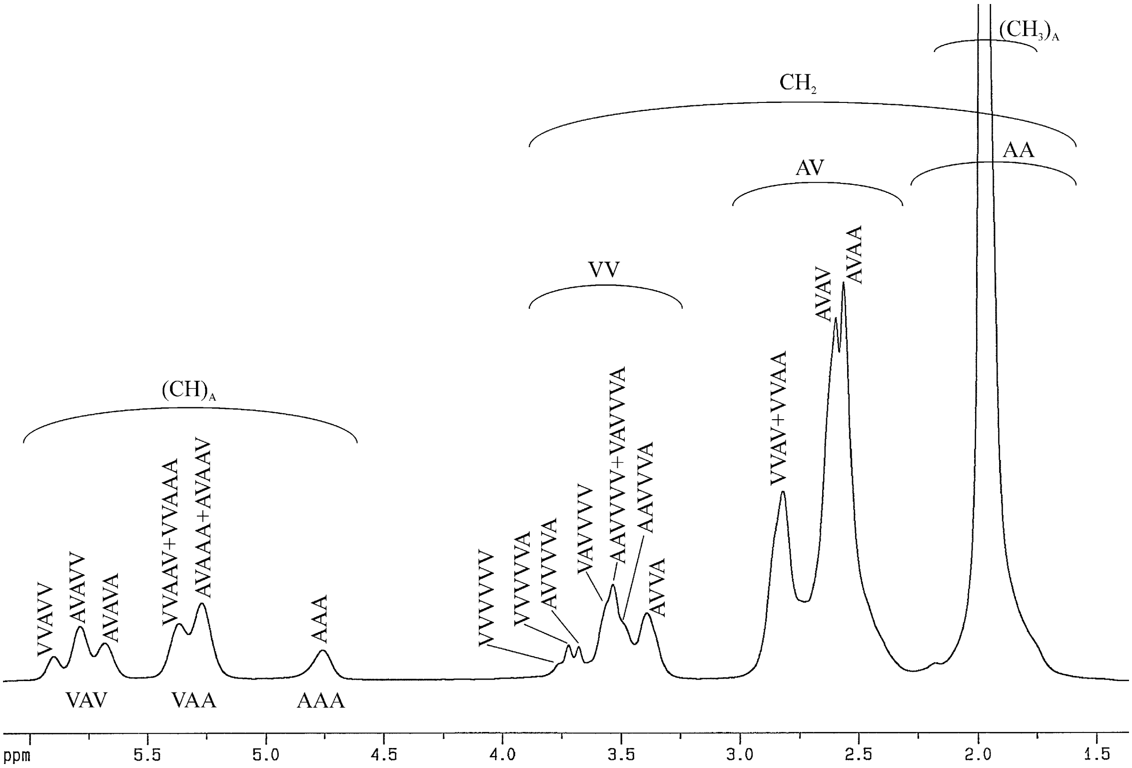

Fig. 4. Assigned ^{1}H spectrum of poly(vinylidene chloride-*co*-vinyl acetate).

between the experimental and simulated spectra substantiated the validity of the approach.

3.3. HSQC spectral analysis

Cross-peaks assigned from the 2D HSQC spectrum (Fig. 7) of copolymer with composition $F_V = 0.52$ are listed in Table 3. Cross-peaks 1–6 were assigned to the couplings between carbon and proton nuclei of methine group of vinyl acetate unit on comparing with the HSQC spectrum of poly(vinyl acetate). Cross-peaks 1, 2 and 3 were assigned to the VVAVV, AVAVV and AVAVA pentads, respectively, by analyzing variation in the intensities of proton resonances and cross-peaks with composition. The vinylidene chloride unit at β and δ position relative to the methine proton impart chemical shift increment to it, thereby as more number of V units gets incorporated at β or δ position the chemical shift of proton increases. Following the reasons stated above, cross-peaks 4 and 5 assigned to the VAA triad were attributed to VVAAV and AVAAA

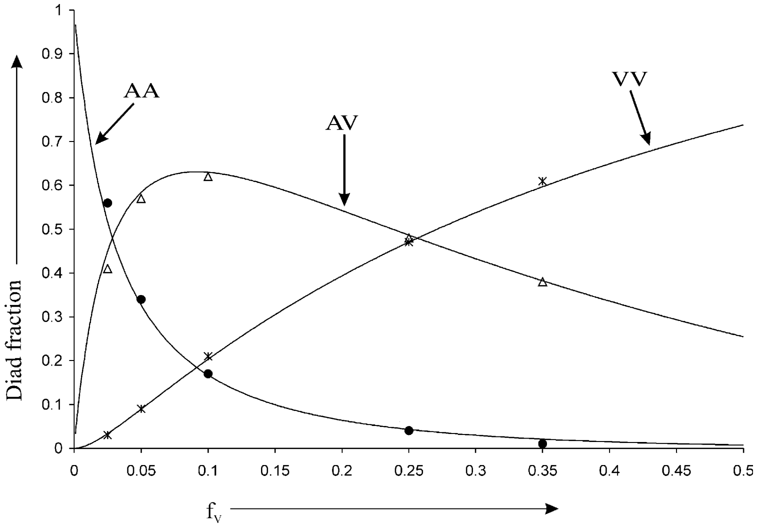

Fig. 5. Variation of the theoretical and experimental diad fractions with change in the infeed of copolymer system.

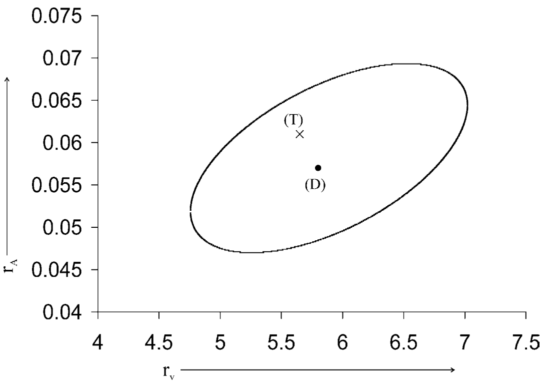

Fig. 6. Joint confidence interval for poly(vinylidene chloride-*co*-vinyl acetate) about the best set of reactivity ratios, $r_V = 5.80$ and $r_A = 0.057$ optimized from diad fractions. The points labeled by D and T are the reactivity ratios optimized by diad and triad fractions, respectively.

pentads, respectively. The assignments of VVAAA and AVAAV pentads could not be ascertained as HSQC spectral analysis could not resolve them.

Cross-peaks 7–14 were assigned to the methylene resonances. Cross-peaks 7, 8 and 9 were assigned to the VVVVVV, AVVVVV and AVVVVA hexads, respectively. Cross-peaks 10 and 11 were attributed to AVVV and AVVA tetrads, respectively. The cross-peaks 12 and 13 were assigned to the VA methylene resonances. Following the analogy of methine resonances of VAA triad centered given above, the cross-peaks 12 and 13 were attributed to the VVAV and AVAA tetrads, respectively. The VVAA and AVAV tetrads could not be differentiated. It was observed that with the increase in the incorporation of vinylidene chloride unit in the compositional sequences, the dispersion of chemical shift of the proton resonances also increases. Cross-peaks 6 and 14 were assigned to methine and methylene of AAA and AA sequences, respectively, by comparison with the HSQC spectrum of poly(vinyl acetate).

3.4. TOCSY spectral analysis

2D TOCSY spectral analysis was carried out to resolve the resonances which could not be assigned using HSQC spectral analysis. Cross-correlation peaks assigned from the TOCSY spectrum given in Fig. 8 are listed in the Table 3. The cross-correlation peak I was assigned to the coupling between the methine proton of VVAVV pentad with the methylene proton of the VVAV tetrad. The coupling is marked as I in Scheme 1(a). The cross-correlation peaks II and III were corresponding to the methine proton of AVAVV pentad which can show couplings with methylene protons of the VAVV and AVAV tetrads (Scheme 1(b)). The chemical shift of cross-correlation peak II on the F_1 axis, corresponding to the methylene proton was same for the cross-peak 12 on HSQC spectrum which was assigned to VAVV tetrad. Thus cross-correlation peaks II and III were assigned to the couplings, marked as II and III, respectively, in Scheme 1(b), between methine proton of AVAVV pentad and methylene protons of VAVV and AVAV tetrads, respectively. The cross-correlation peak IV was assigned to the methine proton of AVAVA pentad which can couple (depicted by couplings labeled IV in Scheme 1(c)) only with the methylene protons of AVAV tetrad. Thus same results were obtained for the assignment of methylene proton of AVAV tetrad independently from HSQC and TOCSY spectral analysis. The TOCSY spectral analysis thus established the assignments of the VVAA and AVAV methylene proton resonances and hence cross-peaks 12 and 13 (Table 3) of the HSQC spectrum. The assigned proton resonances of AV centered tetrads are shown in Fig. 4.

The cross-correlation peak V can be due to the coupling of methylene protons of either VVAA or VVAV tetrad with methine protons. Similarly the cross-correlation peak VI can be attributed to the methylene protons of either AVAA or AVAV tetrad. The methine protons corresponding to the cross-correlation peaks V and VI are of VAA triad centered pentads. Hence the analogous methylene protons should be of the compositional sequences containing VAA sequence, thereby eliminating VVAV and AVAV tetrads for consideration. Methylene protons of the VVAA tetrad can show couplings with methine protons of either VVAAV or VVAAA pentads and methylene protons of the AVAA tetrad can be coupled with either AVAAV or AVAAA pentad. This reasoning ascertained that cross-correlation peak V to be assigned to the coupling between methine proton of VVAAV or VVAAA pentad with methylene protons of the VVAA tetrad and cross-correlation peak VI to the coupling between methine protons of the AVAAV or AVAAA pentads with methylene protons of the AVAA tetrad. This enabled the assignments of the proton resonances of VVAAA and AVAAV pentad sequences (Fig. 4) and hence cross-peaks 4 and 5 in HSQC spectrum. Cross-correlation peaks VII, VIII and IX were assigned to the couplings between methylene protons of AA centered tetrads with methine protons.

The 2D TOCSY spectrum consequently enabled the complete proton resonance assignments in conformity with the 2D HSQC spectral analysis. The usage of homo-nuclear correlation along with the hetero-nuclear correlation proved to be a powerful tool for the NMR analysis.

Table 2
Optimized chemical shift additive parameters for the quaternary carbon of vinylidene chloride in poly(vinylidene chloride-*co*-vinyl acetate)

Parameter	αV	γV	γA	εV(V)	εV(A)	εA(A)	εA(V)	Q
Value of parameter (ppm)	64.98	−5.58	−3.79	0.18	0.15	0.72	0.19	0.52

Table 3

Hetero-nuclear (^{13}C–^{1}H) and homo-nuclear (^{1}H–^{1}H) couplings analyzed from HSQC, TOCSY and HMBC spectra and; chemical shift analysis of quaternary carbon resonances from chemical shift modeling

Copolymer sequence[a]	Group[a]	HSQC assignments			δ ^{13}C[b] (C)			Couplings of nuclei[c] with nuclei[d] analyzed from HMBC and TOCSY spectrum							
		Cross-peak	δ ^{13}C	δ ^{1}H	Peak	Exp	Calc	Nuclei[c]	Spectrum	Cross-peak	Copolymer sequence[e]	Group[e]	Nuclei[d]	δ[c]	δ[d]
VVAVV	CH	1	67.71	5.90				^{1}H	HMBC	1′	AV	CH$_2$	^{13}C	5.90	52.17
								^{1}H	TOCSY	I	VVAV	CH$_2$	^{1}H	5.90	2.86
AVAVV	CH	2	67.66	5.79				^{1}H	HMBC	2′	AV	CH$_2$	^{13}C	5.79	52.17
								^{1}H	TOCSY	II	VAVV	CH$_2$	^{1}H	5.79	2.86
								^{1}H	TOCSY	III	AVAV	CH$_2$	^{1}H	5.80	2.59
AVAVA	CH	3	67.53	5.68				^{1}H	HMBC	3′	AV	CH$_2$	^{13}C	5.68	52.17
								^{1}H	TOCSY	IV	AVAV	CH$_2$	^{1}H	5.68	2.56
VVAAV	CH	4	67.53	5.36				^{1}H	HMBC	23′	VVVAA	C	^{13}C	5.37	86.85
								^{1}H	TOCSY	V	VVAA	CH$_2$	^{1}H	5.36	2.82
								^{1}H	TOCSY	VII	VAAV	CH$_2$	^{1}H	5.36	2.00
VVAAA	CH	4	67.53	5.36				^{1}H	HMBC	23′	VVVAA	C	^{13}C	5.37	86.25
								^{1}H	TOCSY	V	VVAA	CH$_2$	^{1}H	5.36	2.82
AVAAA	CH	5	67.32	5.27				^{1}H	TOCSY	VI	AVAA	CH$_2$	^{1}H	5.27	2.59
								^{1}H	TOCSY	VIII	VAAA	CH$_2$	^{1}H	5.27	1.91
AVAAV	CH	5	67.32	5.27				^{1}H	TOCSY	VI	AVAA	CH$_2$	^{1}H	5.27	2.59
VAA	CH	4+5						^{1}H	HMBC	17′	VAAV	CH$_2$	^{13}C	2.02	67.55
AAA	CH	6	66.85	4.76				^{13}C	HMBC	18′	VAAA	CH$_2$	^{1}H	66.82	1.93
								^{1}H	TOCSY	IX	AAAA	CH$_2$	^{1}H	4.76	1.82
VVVVVV	CH$_2$	7	61.92	3.75				^{1}H	HMBC	7′	VVVV	CH$_2$	^{13}C	3.75	61.91
								^{1}H	HMBC	25′	VVV	C	^{13}C	3.75	83.98
VVVVVA	CH$_2$	8	61.92	2.72				^{1}H	HMBC	8′	VVVV	CH$_2$	^{13}C	3.72	61.91
								^{1}H	HMBC	9′	VVVA	CH$_2$	^{13}C	3.71	62.25
								^{1}H	HMBC	26′	VVV	C	^{13}C	3.72	83.98
AVVVVA	CH$_2$	9	61.92	3.68				^{1}H	HMBC	10′	VVVA	CH$_2$	^{13}C	3.68	62.22
								^{1}H	HMBC	27′	VVV	C	^{13}C	3.68	83.98
AVVV	CH$_2$	10	62.20	3.53											
AVVA	CH$_2$	11	62.20	3.39				^{1}H	HMBC	4′	AV	CH$_2$	^{13}C	3.39	52.17
VVAV	CH$_2$	12	52.17	2.84				^{1}H	HMBC	5′	AV	CH$_2$	^{13}C	2.84	52.17
								^{1}H	HMBC	11′	VV	CH$_2$	^{13}C	2.86	62.23
								^{1}H	HMBC	13′	VAV	CH	^{13}C	2.86	67.50
VVAA	CH$_2$	12	52.17	2.84				^{1}H	HMBC	12′	VV	CH$_2$	^{13}C	2.82	62.23
								^{1}H	HMBC	14′	VAA	CH	^{13}C	2.82	67.50
								^{1}H	HMBC	35′	AAVVV/ AAVVA	C	^{13}C	2.83	86.84
AVAA	CH$_2$	13	52.17	2.57				^{1}H	HMBC	16′	VAA	CH	^{13}C	2.56	67.60
AVAV	CH$_2$	13	52.17	2.57				^{1}H	HMBC	6′	AV	CH$_2$	^{13}C	2.57	52.17
								^{1}H	HMBC	15′	VAV	CH	^{13}C	2.59	67.29
AA	CH$_2$	14	40.1	2.9											
AVVVA	C				1	83.99	83.98								
AVVVV	C				1	83.99	83.99								
VVVVV	C				1	83.99	84.00								

VVV	C	1			^{13}C	HMBC	28′	VAVVVV	CH_2	^1H	83.98	3.58
					^{13}C	HMBC	29′	VAVVVA/AAVVVV	CH_2	^1H	83.98	3.53
					^{13}C	HMBC	30′	AAVVVA	CH_2	^1H	84.02	3.46
VAVVV	C	2	86.25	86.26	^{13}C	HMBC	19′	VVAVV	CH	^1H	86.27	5.90
					^{13}C	HMBC	20′	AVAVV	CH	^1H	86.25	5.78
					^{13}C	HMBC	31′	VAVVVV	CH_2	^1H	86.25	3.58
VAVVA	C	3	86.25	86.27	^{13}C	HMBC	19′	VVAVV	CH	^1H	86.27	5.90
					^{13}C	HMBC	20′	AVAVV	CH	^1H	86.25	5.78
					^{13}C	HMBC	34′	AVVA	CH_2	^1H	86.30	3.39
AAVVV	C	4	86.85	86.83	^{13}C	HMBC	23′	VVAAV/VVAAA	CH	^1H	86.85	5.37
					^{13}C	HMBC	32′	AAVVVV/VAVVVA	CH_2	^1H	86.81	3.53
					^{13}C	HMBC	33′	AAVVVA	CH_2	^1H	86.85	3.49
AAVVA	C	5	86.85	86.84								
VAVAV	C	6	87.52	87.51	^{13}C	HMBC	21′	AVAVV	CH	^1H	87.51	5.80
					^{13}C	HMBC	36′	AVAV	CH_2	^1H	87.51	2.60
AAVAV	C	7	88.07	88.08	^{13}C	HMBC	22′	AVAVA	CH	^1H	88.05	5.68
AAVAA	C	8	88.64	88.64	^{13}C	HMBC	24′	AVAAA/AVAAV	CH	^1H	88.68	5.25
					^{13}C	HMBC	37′	AVAA	CH_2	^1H	88.65	2.55

C, CH and CH_2 represent quaternary carbon, methine and methylene groups, respectively.

[a,c,d,e] Couplings between nuclei[c] (^1H or ^{13}C) of the group[a] belonging to the copolymer sequence[a] and nuclei[d] (^1H or ^{13}C) of the group[e] belonging to the copolymer sequence[e] analyzed from the TOCSY and HMBC spectral analysis. Chemical shifts of the cross-peaks corresponding to the nuclei[c] and nuclei[d] are listed as δ^c and δ^d, respectively.

[b] Listing of quaternary carbon resonances peak no. (Fig. 2) experimental (exp) and calculated (calc) chemical shifts.

Table 4
Concentration of quaternary carbon centered pentads of poly(vinylidene chloride-*co*-vinyl acetate)

	$F_V=0.35$		$F_V=0.25$		$F_V=0.10$		$F_V=0.05$		$F_V=0.03$	
	Exp	Calc	Exp	Calc	Exp	Calc	Exp	Calc	Exp	Calc
VVVVV										
AVVVV	0.57	0.57	0.43	0.43	0.14	0.15	0.05	0.06	0.01	0.01
AVVVA										
VAVVV	0.35	0.33	0.26	0.25	0.11	0.12	0.17	0.19	0.04	0.06
VAVVA			0.13	0.13	0.19	0.19				
AAVVV	0.02	0.03	0.03	0.05	0.06	0.06	0.21	0.19	0.18	0.15
AAVVA	0.02	0.01	0.04	0.02	0.13	0.10				
VAVAV	0.03	0.05	0.07	0.09	0.14	0.16	0.11	0.14	0.04	0.06
AAVAV	0.01	0.01	0.04	0.03	0.16	0.17	0.27	0.28	0.28	0.32
AAVAA	0.00	0.00	0.00	0.00	0.07	0.05	0.19	0.14	0.45	0.41

3.5. HMBC spectral analysis

2D HMBC spectral analysis was done to establish the assignments done from the HSQC and TOCSY spectrum. The 2D HMBC (Fig. 9) assignments are given in the Table 3. Cross-peaks 1′, 2′ and 3′ were assigned to the couplings between methylene carbon of AV diad with the methine protons of the VVAVV, AVAVV and AVAVA, respectively. Coupling 3′ corresponding to the cross-peak 3′ is depicted in the Scheme 1(c). Cross-peaks 5′ and 6′ were due to the couplings between methylene carbon of AV diad and methylene protons of the adjacent AV diad centered tetrad, thus indicating the presence of either VAV or AVA sequence in the tetrads corresponding to the proton resonances. The cross-peaks 5′ and 6′ were therefore assigned to the couplings between methylene carbon of the AV diad with the methylene protons of the VVAV and AVAV tetrads, respectively. HMBC spectral analysis hence resolved the VVAV and AVAV tetrads thereby establishing their assignments. The couplings corresponding to the cross-peaks 5′ and 6′ are schematically presented as couplings 5′ (Scheme 1(a) and (b)) and 6′ (Scheme 1(b) and (c)).

Cross-peaks 7′ and 8′ were assigned to the couplings between methylene carbon of VVVV tetrad with methylene protons of VVVVVV and AVVVVV hexads, respectively. Similarly cross-peaks 9′ and 10′ were assigned. The cross-peaks 7′–10′ enabled to assign the proton resonances of VVVV centered sequences at hexad level of compositional sensitivity (Table 3). Cross-peaks 11′ and 12′ were

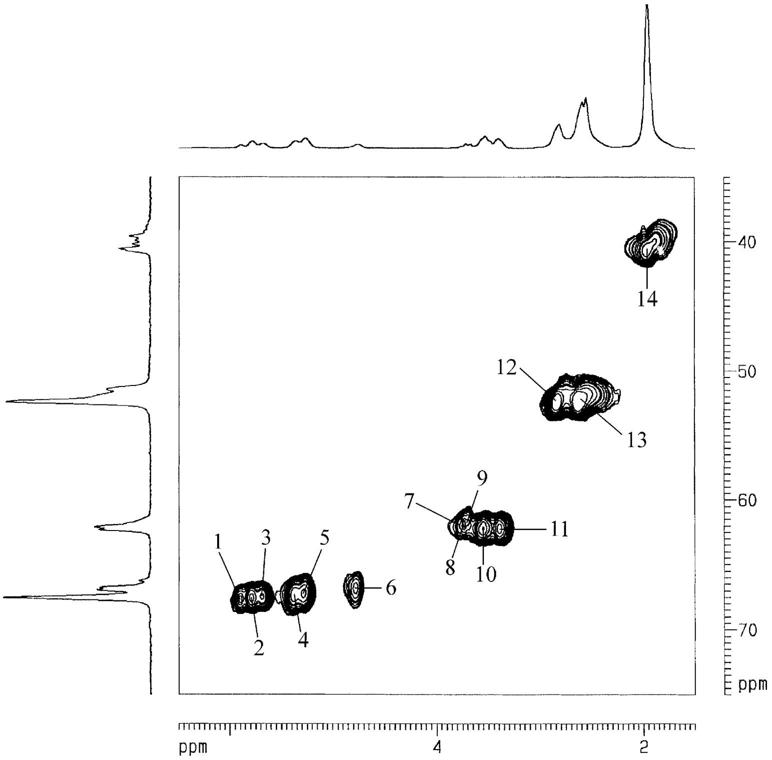

Fig. 7. 2D HSQC spectrum of poly(vinylidene chloride-*co*-vinyl acetate) of composition $F_V=0.52$.

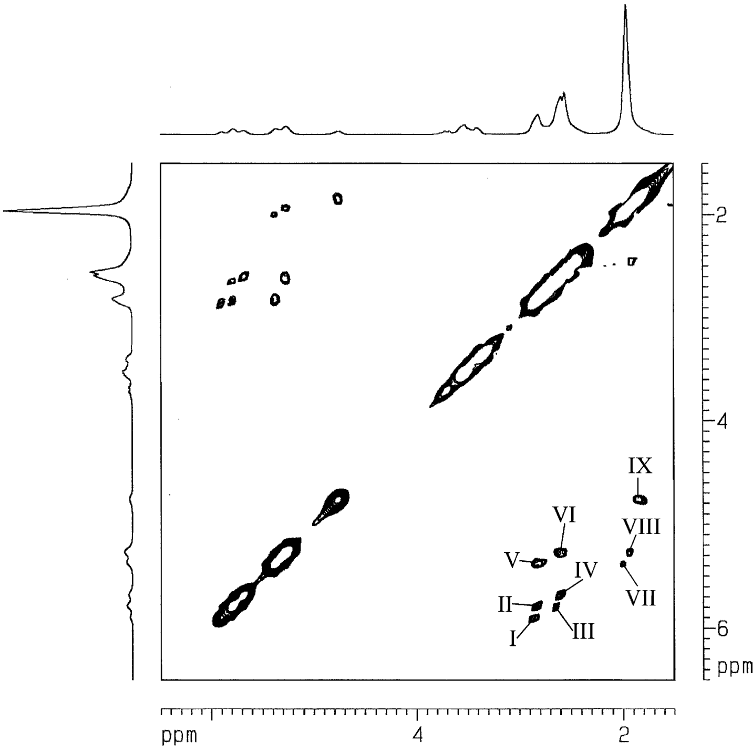

Fig. 8. 2D TOCSY spectrum of poly(vinylidene chloride-*co*-vinyl acetate) of composition $F_V = 0.52$.

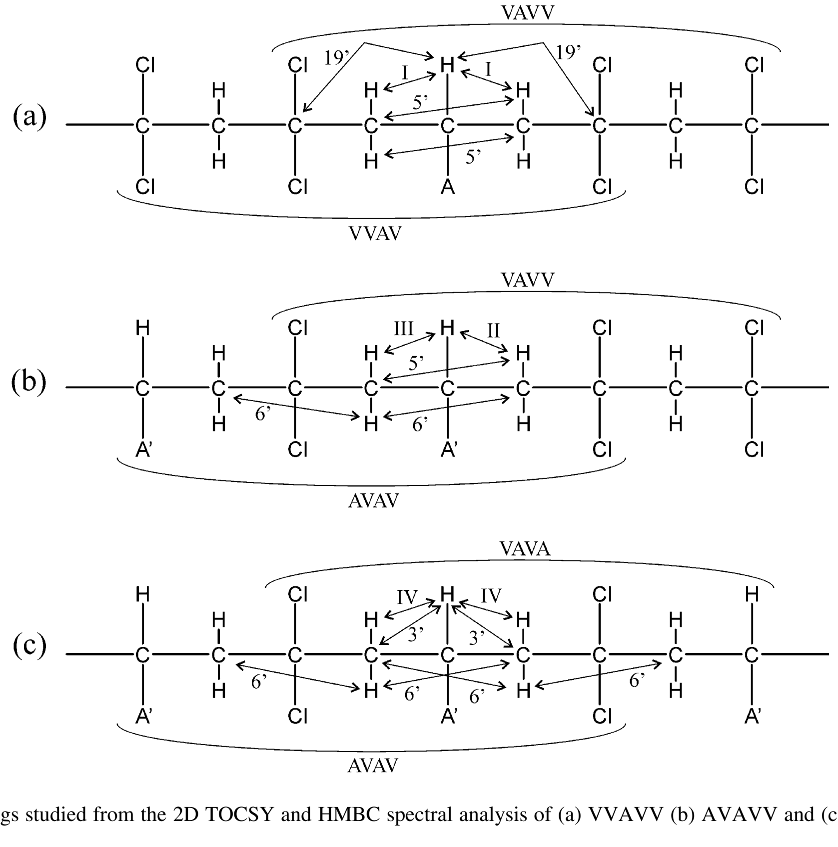

Scheme 1. Couplings studied from the 2D TOCSY and HMBC spectral analysis of (a) VVAVV (b) AVAVV and (c) AVAVA pentads.

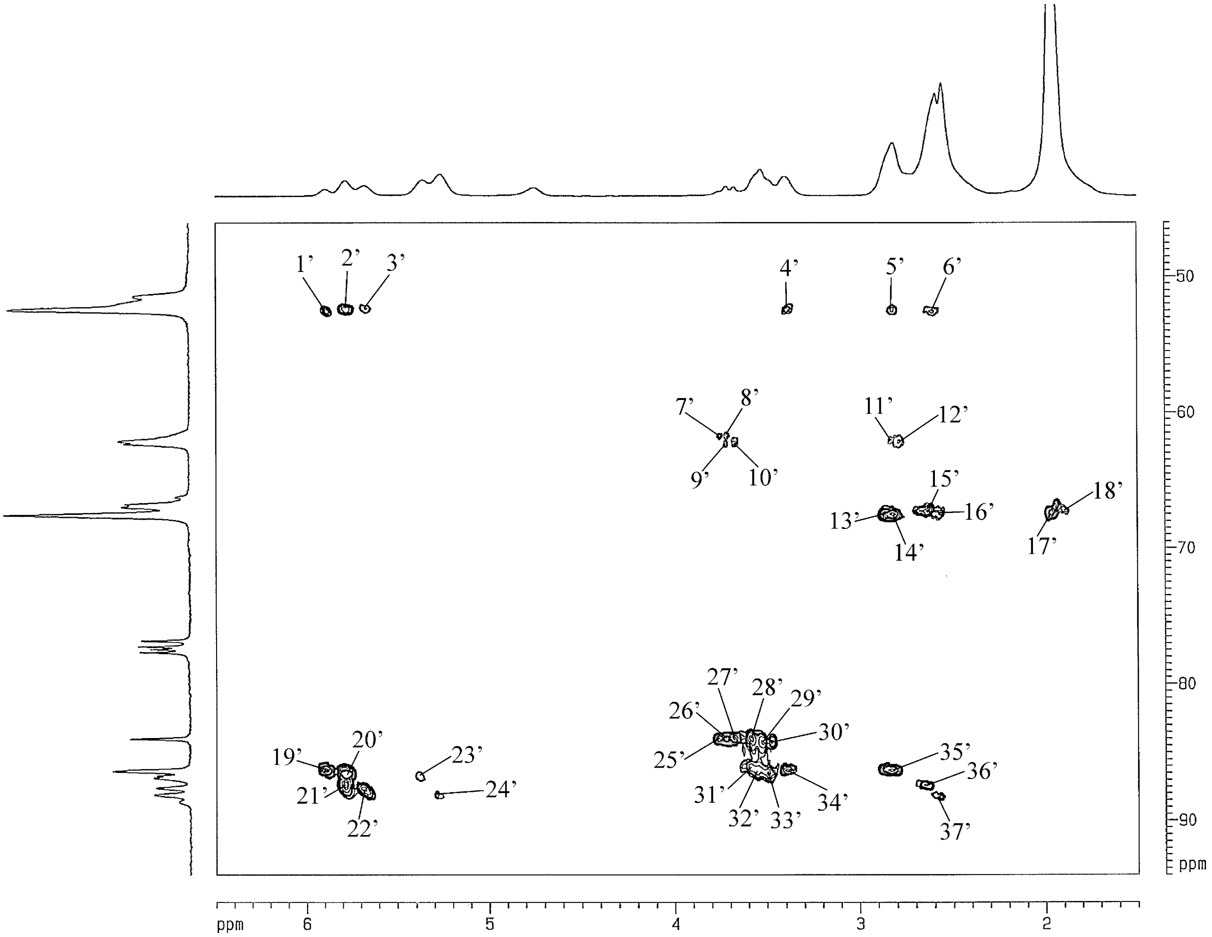

Fig. 9. 2D HMBC spectrum of poly(vinylidene chloride-*co*-vinyl acetate) of composition $F_V = 0.52$.

corresponding to the coupling between methylene carbon of VV diad and methylene protons of the VA diad centered tetrads. Methylene carbon of VV diad can couple with the methylene protons of only those tetrads, which contain VV sequence. Only VVAV and VVAA tetrads (of VA centered diads) contain the sequence VV and AVAA or AVAV tetrads do not have the VV sequence. Consequently attributing cross-peaks $11'$ and $12'$ to the couplings between methylene carbon of VV diad with methylene protons of VVAV and VVAA tetrads, respectively, thereby establishing the assignments of the VVAA and AVAV proton resonances. Cross-peaks $13'$–$18'$ were assigned to the couplings between methine carbon and methylene protons as given in the Table 3.

Cross-peak $19'$ was corresponding to the methine proton of the VVAVV pentad which can show coupling to the quaternary carbon of the unit containing the sequence VVAV, as shown by couplings labeled $19'$ in Scheme 1. Also, the quaternary carbon corresponding to the cross-peak was of VVA triad. The sequence VVAV along with being VVA centered can be present only in the VAVVV or VAVVA pentads, thus cross-peak $19'$ was assigned to the coupling of methine proton of VVAVV pentad with the quaternary carbon of VAVVV or VAVVA pentads. The cross-peak $20'$ was corresponding to the methine proton of the AVAVV pentad and quaternary carbon of VVA triad. The methine proton of AVAVV sequence can show coupling with the quaternary carbon of pentad containing either AVAV or VAVV sequence. Now as AVAV sequence does not contain the VVA sequence, thus only VAVV sequence was left for consideration and hence the cross-peak $20'$ was assigned to the coupling between methine proton of the AVAVV pentad and quaternary carbon of either VAVVV or VAVVA pentads. Following this logic, the rest of the cross-peaks due to the couplings between methine proton and quaternary carbon, i.e. $21'$–$24'$ were assigned to the three bond order couplings between methine proton and quaternary carbon.

Cross-peaks $25'$–$37'$, listed in the Table 3 were due to the couplings between quaternary carbon and methylene protons. Cross-peaks $28'/31'$, $29'/32'$ and $30'/33'$ assigned to the couplings between the methylene protons of VAVVVV, AAVVVV/VAVVVA and AAVVVA, respectively, with the quaternary carbons as given in Table 3. These cross-peaks facilitated in the assignments of the AVVV centered tetrads up to the hexad level of compositional sensitivity. The cross-peaks justified the assignments of the quaternary carbon done by the chemical shift modeling and the assignments of the methylene protons done with the help of 2D HSQC and 2D TOCSY spectral analysis. The proton spectrum assigned with the help of the HSQC, TOCSY and HMBC spectral analysis is given in the Fig. 8.

4. Conclusions

The methodology based on the chemical shift modeling, spectral simulation and two-dimensional homo-nuclear and hetero-nuclear NMR spectroscopic techniques was applied for the microstructure analysis of poly(vinylidene chloride-*co*-vinyl acetate). Reactivity ratios optimized from the diad fractions ($r_V = 5.80$ and $r_A = 0.057$) and from triad fractions ($r_V = 5.65$ and $r_A = 0.061$) were in good agreement. The chemical shift modeling of the assigned quaternary resonances signals enabled to predict the chemical shifts of the unassigned overlapping resonances at pentad level. 2D HSQC, TOCSY and HMBC spectral analysis helped in the assignments of the methine proton resonances at pentad level of sensitivity. Methylene proton resonances were assigned up to hexad level of compositional sensitivity. The methodology helped to investigate the resonance signals to higher level thus, giving deeper insight into the polymer microstructure.

References

[1] Weixia L, Rinaldi PL, McIntosh LH, Roderic PR. Macromolecules 2001;34:4757.

[2] Oh SJ, Kinney DR, Wang W, Rinaldi PL. Macromolecules 2002;35:2602.

[3] Wyzgoski FJ, Rinaldi PL, McCord EF, Stewart MA, Marshall DR. Macromolecules 2004;37:846.

[4] Xie X, Wittmar M, Kissel T. Macromolecules 2004;37:4598.

[5] Kowalczuk-Bleja A, Trzebicka B, Komber H, Voit B, Dworak A. Polymer 2004;45:9.

[6] Matsuda H, Nagasaka B, Asakura T. Polymer 2003;44:4681.

[7] Subramanyam U, Rajamohanan PR, Sivaram S. Polymer 2004;45:4063.

[8] Brar AS, Singh G, Shankar R. J Mol Struct 2004;703:69.

[9] Chen EYX. J Polym Sci, Part A: Polym Chem 2004;42:3395.

[10] Escher FFN, Galland GB. J Polym Sci, Part A: Polym Chem 2004;42:2474.

[11] Brar AS, Kaur S. J Polym Sci, Part A: Polym Chem 2005;43:1100.

[12] Wiles KB, Bhanu VA, Pasquale AJ, Long TE, McGrath JE. J Polym Sci, Part A: Polym Chem 2004;42:2994.

[13] Ito H, Miller DC. J Polym Sci, Part A: Polym Chem 2004;42:1468.

[14] Bisht HS, Ray SS, Chatterjee AK. J Polym Sci, Part A: Polym Chem 2003;41:1864.

[15] Sakai H, Kodani T, Takayama A, Nomura M. J Polym Sci, Part B: Polym Phys 2002;40:948.

[16] Centeno TA, Fuertes AB. Carbon 2000;38:1067.

[17] Gonzalez A, Iriarte M, Iriondo PJ, Iruin JJ. Polymer 2002;43;6205.

[18] Tamai H, Ogawa J, Yasuda H. J Colloid Interface Sci 2003;260:312.

[19] Tamai H, Kouzu M, Yasuda H. Carbon 2002;411:1645.

[20] Kim YJ, Horie Y, Ozaki S, Matsuzawa Y, Suezaki H, Kim C, et al. Carbon 2004;42:1491.

[21] Tamai H, Kunihiro M, Yasuda H. J Colloid Interface Sci 2004;275:44.

[22] Cheng HN, Bennett MA. Anal Chem 1984;56:2320.

[23] Cheng HN. J Chem Inf Comput Sci 1987;27:8.

[24] Cheng HN. Polym News 2000;25:114.

[25] Nguyen G, Nicole D, Swistek M, Matlengiewicz M, Wiegert B. Polymer 1997;38:3455.

[26] Matlengiewicz M, Nguyen G, Nicole D, Itenzeu N. J Polym Sci, Part A: Polym Chem 2000;38:2147.

[27] Brar AS, Singh G, Shankar R. Eur Polym J 2005;41:747.

[28] Brar AS, Singh G, Shankar R. Eur Polym J 2004;40:2679.

[29] van Herk AM. J Chem Educ 1995;72:138.

[30] van Herk AM, Dröge T. Macromol Theory Simul 1997;6:1263.

[31] Dutta K, Mukherjee M, Brar AS. J Polym Sci, Part A: Polym Chem 1999;37:551.

[32] Brar AS, Malhotra M. Macromolecules 1996;29:7470.

[33] Brar AS, Hekmatyar SK. J Appl Polym Sci 2001;79:544.